Appl Biochem Biotechnol (2013) 171:731–743
DOI 10.1007/s12010-013-0368-y

Cell Morphology Variations of *Klebsiella pneumoniae* Induced by Acetate Stress Using Biomimetic Vesicle Assay

Shengguo Lu · Yuwang Han · Xujia Duan · Fang Luo · Lingyan Zhu · Shuang Li · He Huang

Received: 15 April 2013 / Accepted: 23 June 2013 /
Published online: 28 July 2013

Abstract Supplementation with acetate under low levels was used as a novel approach to control the morphological development of *Klebsiella pneumoniae* aimed to improve 1,3-propanediol (1,3-PD) production. A full range of morphological types formed from rod shape to oval shape even round shape in response to different concentrations of acetate. The cell growth and 1,3-PD productions in the shake flasks with 0.5 g/L acetate addition were improved by 9.4 and 28.37 %, respectively, as compared to the control, while the cell became shorter and began to lose its original shape. The cell membrane penetration by acetate was investigated by the biomimetic vesicles, while higher concentration of acetate led to more moderate colorimetric transitions. Moreover, the percentage composition of unsaturated fatty acid (UFA) was increased as well as the increased concentrations of acetate, whereas higher UFA percentage, higher fluidity of bacterial cell membrane.

Keywords Acetate stress · Biomimetic vesicle assay · 1,3-Propanediol · Cell morphology · *Klebsiella pneumoniae* · Membrane phospholipids analysis

Introduction

Recent advances in the morphology engineering of filamentous microorganisms have shown that the productivity in biotechnological processes was often correlated with the morphological form [1, 2]. However, there is only little literature on the correlation between bacterial morphology and productivity in biosynthesis process. In view of the high importance of morphology, it is worth manipulating the proper bacterial morphology for good performance in biotechnological process.

Biosynthesis of 1,3-propanediol (1,3-PD) can be achieved with low-cost renewable glycerol as a substrate, which has recently attracted worldwide interests. This is because 1,3-PD is not only a versatile degradable intermediate compound for heterocycle synthesis

S. Lu · X. Duan · F. Luo · L. Zhu · S. Li · H. Huang (✉)
State Key Laboratory of Materials-Oriented Chemical Engineering, College of Biotechnology and Pharmaceutical Engineering, Nanjing University of Technology, No. 5 Xinmofan Road, Nanjing, Jiangsu 210009, People's Republic of China
e-mail: biotech@njut.edu.cn

Y. Han
College of Science, Nanjing University of Technology, No. 5 Xinmofan Road, Nanjing, Jiangsu 210009, People's Republic of China

but also a monomer for polymer production [3]. *Klebsiella pneumoniae* is a preferred fermenting organism in the 1, 3-PD-producing industry due to its high inhibitor tolerance and 1, 3-PD productivity [4]. However, the fermentation is also affected by both inhibitory process products. Acetate is one of the major inhibitory products during 1,3-PD biosynthesis process [5]. It is widely accepted that the toxicity of acetate is well manifested by its effect on cell integrity and membrane composition [6]. Interestingly, our group used agricultural residues to improve 1,3-PD production and showed that one of degradation products, acetate with low level, can effectively stimulate cell growth of *K. pneumoniae* and 1,3-PD production [7]. The improved 1,3-PD production maybe due to the cell morphology induced by acetate.

Acetate may have toxic or beneficial effects on cell functions and phenotypes, but such effects have been not well understood. Therefore, it is necessary to understand the mechanism of the acetate stress in order to design and optimize the positive stimulating effect of acetate on 1,3-PD fermentation.

Unfortunately, investigating the inhibitor interactions with the structural, functional and mechanistic aspects of the membrane process is still a major challenge due to the complexity of physiological membrane. Few studies have demonstrated how the acetate affects cell membrane [6]. Over years, a wide variety of model membrane systems have been developed, providing insights into biological processes on membrane surfaces or within membrane lipid bilayers. Biomimetic vesicles composed of polydiacetylene (PDA) act as a vehicle for biological sensing, which have been a useful platform for rapid screening membrane processes and biomolecular recognition events [8]. These PDA-based biomimetic vesicles can act as a "scaffolding" for stabilization of lipid bilayers or entire membrane domains. Meanwhile, it can serve as a transduction vehicle for generating color/fluorescence signals induced by membrane-associated events. Lipid/PDA vesicle systems have been used to study membrane interactions of short antimicrobial peptides, and the penetration degree of the peptides into lipid bilayers is measured by the percentage of colorimetric response (CR) [9–11].

The present work dealt with sodium acetate addition for controlling the morphology of *K. pneumoniae* and studied the correlation between cell morphology and 1,3-PD biosynthesis process in detail. The polydiacetylene-based colorimetric assay was constructed to quantitatively determine the acetate stress in membrane penetration. After comparison of membrane's fatty acid profile from the strains in response to different levels of acetate, the modification of phospholipid compositions and unsaturation ratios adapted to different acetate stresses were observed. Taken together, the results suggested that modification of cell membranes in response to the acetate stress with low level could enhance the cell growth and 1,3-PD biosynthesis.

Materials and Methods

Materials

The diacetylenic monomer 10,12-pentacosadiynoic acid (PCDA) at a purity of 98 % was purchased from Alfa Aesar, washed in chloroform, and passed through a 0.45-μm nylon filter prior to use. Polymixin-B (PMB) sulfate was purchased from Sigma.

Strains, Growth Conditions, and Analytical Methods

The strain for 1,3-PD production used in this study was *K. pneumoniae* ME-303 [7] from *K. pneumonia*e ATCC 25955 by mutagenesis (*K. pneumoniae*), obtained from Nanjing University of Technology.

The seed medium consisted of 3.0 g/L yeast extract, 3.0 g/L malt, 5.0 g/L peptone, and 5.0 g/L NaCl. The fermentation medium was composed of 5 g/L yeast extract, 10 g/L $K_2HPO_4 \cdot 3H_2O$, 2 g/L KH_2PO_4, 1 g/L NH_4Cl, 0.5 g/L NaCl, 0.1 g/L $MgSO_4 \cdot 7H_2O$, 30 mg/L $FeCl_3 \cdot 6H_2O$, 5 mg/L $CoCl_2 \cdot 6H_2O$, 5 mg/L vitamin B_{12}, and 30 g/L glycerol. In order to prepare the inoculums, a 100-mL seed medium was inoculated with *K. pneumoniae* in an Erlenmeyer flask (250 mL). The flasks were then incubated at 37 °C and 140 rpm for 10 h and subsequently inoculated into Erlenmeyer flasks at 5 % (*v*/*v*). The flask fermentation was carried out in 250-mL Erlenmeyer flasks containing 100 mL fermentation medium with cultivation at initial pH 7.0, 37 °C, and 140 rpm for 15 h.

1,3-PD, acetic acid, 2,3-butanediol, lactic acid, alcohol, succinic acid, and xylose were analyzed by using a high-performance liquid chromatography system (Dionex with a Bio-Rad HPX-87H ion exclusion column) with a refractive index detector at 65 °C. H_2SO_4 (0.005 mol/L) was used as mobile phase at a flow rate of 0.8 mL/min. Biomass was determined at 600 nm with appropriate dilution using a UV–visible spectroscopy system (Perkin Elmer Lambda 25, USA).

Scanning Electron Microscopy Image

After the treatments, cells were fixed with glutaraldehyde (2.5 %; Sigma Chemical), and then dehydrated in water–alcohol solutions at various alcohol concentrations (30, 50, 70, 80, 90, and 100 %) and in amyl acetate–alcohol solutions (30, 50, 70, and 100 %) for 10 min each. After that, samples were dehydrated with a critical point dryer (EMS 850, Electron Microscopy Sciences, Hatfield, PA) at 42 °C and 1,300 psi. Samples were fixed on a SEM support and sprayed with Au-Pd prior to observation using a field emission gun SEM (JSM-5900, Japan Electron Optical Laboratory). The cell length and width were measured with image visualization software Image-J 1.34. Average length and width distributions of cells were determined by three photographs taken for each sample, and each sample with 60 cells was measured from the SEM images.

Phospholipids Extraction from Cell Membrane

Total cellular lipids were extracted based on the method of Xia and Yuan [12]. Cells were separated from medium through filtration immediately after sampling. Then, they were washed by deionized water for three times. Subsequently, the cells were transferred into a fresh glass tube containing 1 mL brine and 1 mL chloroform/methanol (*v*/*v*, 1:1). The mixture was gently shaken for 1 h and then refrigerated at −7 °C overnight. In order to get a three-layer system, the tube was then centrifuged at 376×*g* for 5 min. The chloroform phase was separated, and the remaining methanol/water solution was re-extracted with chloroform. Then, the two chloroform phases were combined, the solvent was removed under reduced pressure at room temperature, and the remaining lipid-containing fraction was freeze-dried. Lipids were stored at 20 °C until use.

GC/MS Analysis

FA methyl esters were analyzed on GC-MS (Thermo Electron Corporation, Trace GC 2000 DSQ, USA) after chemical derivatization. Briefly, 1 μL of sample was injected with splitless injection into GC, which was equipped with a fused silica capillary column (30 m×0.25 mm×0.25 μm, DB-5MS, Agilent, USA). The injector temperature was 250 °C. It was operated on constant flow mode at 1 mL/min. Helium was used as carrier gas. The column temperature was maintained at 80 °C for 2 min, then increased to 200 °C with the rate of 40 °C/min, and finally heated to 300 °C

at 10 °C/min and held for 6 min. The temperature of transfer line and ion source was set at 250 and 200 °C, respectively. Ions were generated by a 70-eV electron beam. Mass range was set 50–600 aum.

Vesicle Preparation

The PDA/lipid biomimetic skeletons were prepared with the slightly modified method described in Ma et al. [13]. Then, PCDA was washed in chloroform and passed through a 0.45-μm nylon filter prior to use. The mixed lipids (8 mg lipid extracts from *K. pneumoniae* and 14.98 mg PCDA) were dissolved in 1:1 chloroform/ethanol and dried in a rotatory evaporator. The dry monomer/lipid film was formed. An appropriate amount of distilled water was added to give a PCDA concentration of 1 mM. Subsequently, the sample was probe-sonicated in deionized water at 70 °C for 30 min and for another 4 min without heating. The vesicle solution was filtered through 0.8-μm nylon filter, then cooled and kept at 4 °C overnight.

UV–Vis Measurements

For analysis of the colorimetric transitions-induced by the acetate stress, PDA/phospholipid vesicles were mixed with various amounts of sodium acetate followed by addition of Tris buffer and filled with water to 1 mL. Final concentrations: vesicles 0.5 mM, Tris 1.5 mM, sodium acetate with different amounts. The pH of all components was maintained at 7.0. All spectroscopic measurements were carried out at room temperature using a UV–vis spectrophotometer (Perkin Elmer Lambda 25, USA). Quantitation of the extent of blue-red color transition was given by the colorimetric response (%CR) [9], defined by $\%CR=(PB_0-PB_I)/PB_0$, where $PB_0=A_{650}/(A_{650}+A_{550})$ for the control and $PB_I=A_{640}/(A_{640}-A_{550})$ for samples (PB_0 is the blue/red ratio of the control sample, and PB_I is the value obtained for the vesicle solution after colorimetric transition occurs).

Results

Influence of Acetate on Cell Morphology

Scanning electron micrographs (Fig. 1) revealed a remarkable change of the morphology for *K. pneumoniae* induced by elevated levels of sodium acetate (after the fermentation run for 15 h). The cells from the control (without the acetate addition) kept original rod shape, and the average length of individual cells was ~1.66 μm (Vs cell width ~0.73 μm; Fig.1a). In contrast, cells from incubation with 0.5 g/L acetate addition showed dramatic changes in morphology (Fig. 1b). The original rod shape was lost, and became shortened in which individual cell length was ~1.14 μm on average (Vs. cell width ~0.74 μm). In addition, smooth structures on the surface were observed. Similar morphological disturbances were observed upon exposure to 1.0 g/L acetate (Fig. 1c).Up to 4 g/L (Fig. 1d), this obviously lost original rod shape and began to create oval shape in place in which the cells had an average length of ~1.06 μm. Furthermore, when challenged at addition of 8 g/L, a significant number of cells kept oval shape, and a few began to form rounded shape (Fig. 1e). The cell length was decreased to ~0.96 μm on average (Vs. cell width ~0.78 μm). Upon the acetate stress at different levels, a range of morphological types from rod shape to oval or round shape were observed, showing that was dependently on the concentration of sodium acetate.

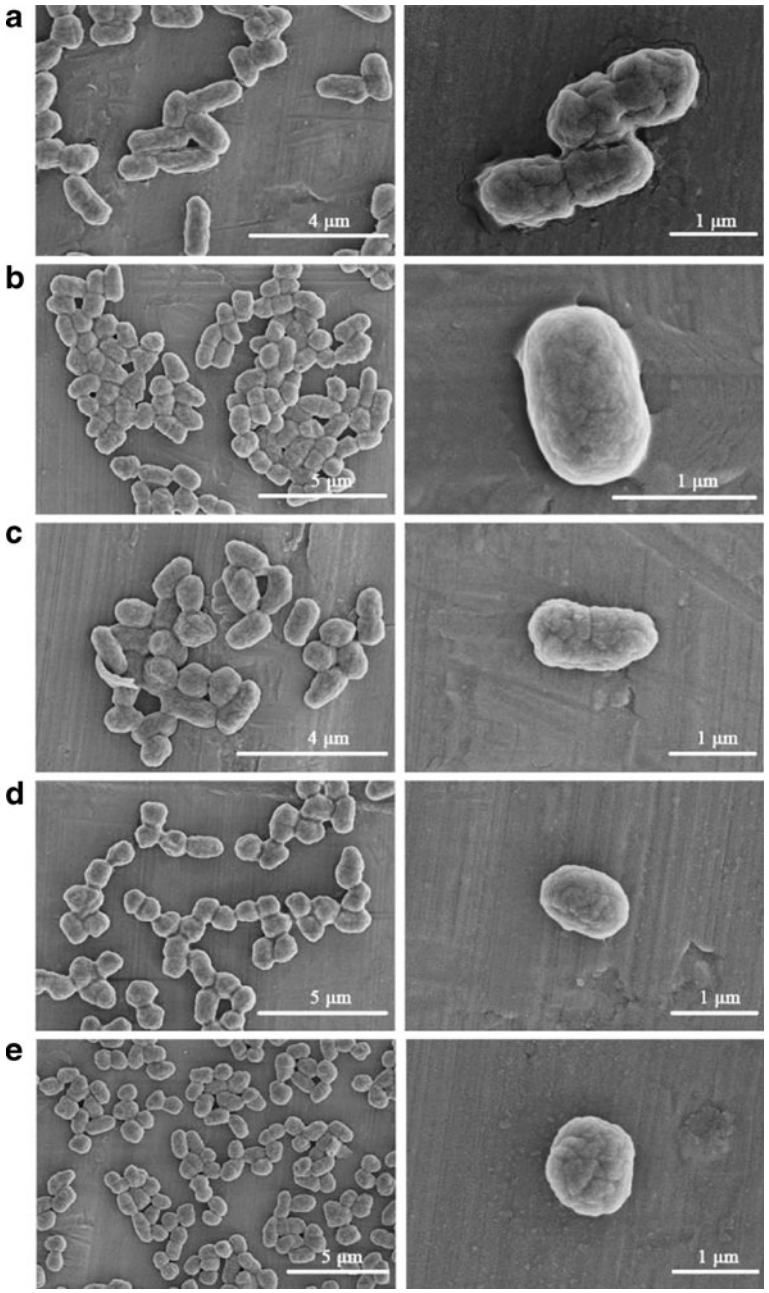

Fig. 1 Scanning electron microphotographs of *K. pneumoniae* in shake flasks. The sodium acetate was added at varied concentrations: control without addition (**a**), 0.5 g/L (**b**), 1.0 g/L (**c**), 4 g/L (**d**), 8 g/L (**e**)

The Acetate Stress on Cell Growth and Biosynthesis Process of *K. pneumoniae*

The effect of sodium acetate on cell growth was investigated first. The cell growth of *K. pneumoniae* showed great variations in the presence of sodium acetate (the pH of initial

fermentation medium was 7.0; Fig. 2). In the presence of acetate, the cell growth kept increasing until the addition of sodium acetate more than 4.0 g/L. The maximum cell concentration was 5.51 (OD_{600}) when *K. pneumoniae* grew in the medium supplemented with 4.0 g/L sodium acetate, which was ~30 % higher than that of the control. However, the cell was inhibited by a further increased concentration of sodium acetate.

In view of the positive effect of sodium acetate on cell growth of *K. pneumoniae*, 1,3-PD fermentation with different concentrations of sodium acetate supply was carried out to determine the effect on the biosynthesis process. As is shown in Fig. 2, 1,3-PD concentration was significantly increased with a small amount of acetate addition and retained the highest level (11.47 g/L) after 0.5 g/L sodium acetate supply, and gradually decreased by further addition of sodium acetate. It was worth noting that the final 1,3-PD productions with 0.5, 1.0, 2.0 g/L addition were 28.37, 19.59, and 5.571 % higher than the control. Another important product in 1,3-PD fermentation, 2,3-butanediol was significantly decreased in the presence of above 1.0 g/L sodium acetate, while it was hardly affected by adding a small amount of sodium acetate (0–1.0 g/L). Interestingly, the ethanol concentration relative to the added sodium acetate was similar to that of 1,3-PD. The ethanol concentration was significantly improved by addition of sodium acetate, and the highest concentration of 4.54 g/L was retained when the sodium acetate was controlled at 2.0 g/L. Subsequently, the ethanol concentration gradually declined with a higher concentration of sodium acetate.

This study also investigated the distribution of acid metabolites (lactic acid, succinic acid, and acetic acid), which are the key by-products during 1,3-PD fermentation. The succinic acid concentration was increased first and then decreased, whereas the total succinic acid concentration kept at a minor level compared with that of other by-products (Fig. 2). The lactic acid biosynthesis was severely inhibited by the addition of sodium acetate. The lowest concentration of lactic acid was 0.155 g/L, and it was approximately 90 % less than that of the control. Considering the additional increment of sodium acetate, the acetic acid biosynthesis was reflected by $\Delta c_{\text{acetate}}$. The $\Delta c_{\text{acetate}}$ was defined as the difference of total acetate concentration (C_t) and additional acetate concentration (C_{add}). Figure 3 shows that the Δacetate was similar to that of the lactic acid biosynthesis process, whereas the more sodium acetate was added, the less $\Delta C_{\text{acetate}}$ was achieved. The Δacetate significantly declined with the additional sodium acetate, and it was decreased from 0.2 to −2.6 g/L. It is important to note that *K. pneumoniae* could have an ability to metabolize the acetate.

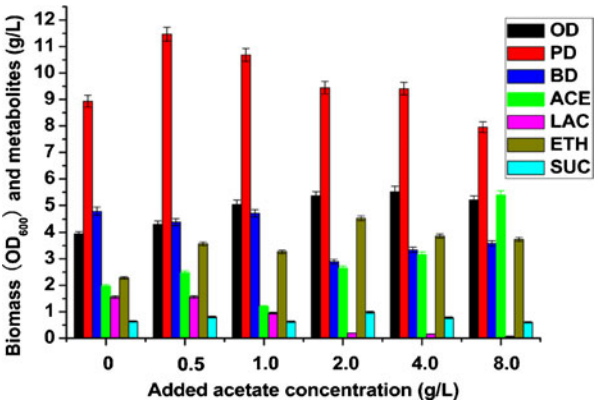

Fig. 2 Effects of acetate with different concentrations on cell growth and 1,3-propanediol biosynthesis process. All the data are the average of three experiments. *OD* biomass, *PD* 1,3-propanediol, *BD* 2,3-butanediol, *ACE* acetic acid, *LAC* lactic acid, *ETH* ethanol, *SUC* succinic acid

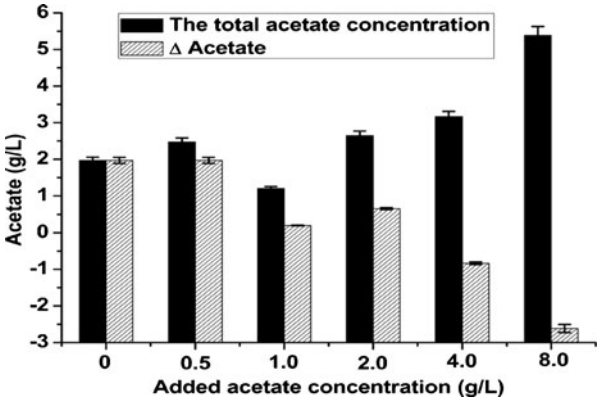

Fig. 3 The relationship between the additional acetate and Δacetate. The $\Delta c_{\text{acetate}}$ was defined as the difference of total acetate concentration (C_t) in the fermentation medium and additional acetate concentration (C_{add})

However, it remains unclear how and when they were metabolized by *K. pneumoniae*. The metabolic pathways of acetic ions by *K. pneumoniae* are investigated in the process. This result suggested that the total amount of acid metabolites was evidently inhibited by the addition of sodium acetate.

The Relation Between Cell Morphology and 1,3-PD Biosynthesis Process

From Fig. 4, the sodium acetate supply affected the cell morphology, biomass, and 1,3-PD production obviously. Under the control without acetate addition, the cell morphology kept rod shape with the highest cell length of ~1.66 μm and the cell length–width ratio of 2.27. Under the control, the biomass and 1,3-PD production were both almost at the lowest level. With 0.5 g/L sodium acetate addition, the cell length became shorter and began to lose its original shape with the length–width ratio of 1.6, whereas the biomass and 1,3-PD production were improved significantly, especially the 1,3-PD production reached a maximum value of more than 11 g/L. Upon the addition of 1.0 g/L sodium acetate, the similar effect on morphology (the cell length–width ratio of 1.56), biomass, and 1,3-PD production was observed. After addition of 4 g/L sodium acetate, the rod shape was generally lost and changed to oval shape in place (the cell length–width ratio of 1.44). The biomass was further increased, whereas the 1,3-PD production declined significantly under this condition. More morphological changes were observed upon 8 g/L sodium acetate supply, the cell length–width was increased to 1.22, while 1,3-PD production decreased further and as well as biomass.

Colorimetric Detection of Acetate–Membrane Interaction

To get further insight into underlying mechanism of interaction between acetate stress and cell membrane, here we present a bioanalytical assay by PDA-based vesicles. Initially, the phospholipid/PDA biomimetic vesicles were used to demonstrate the membrane perturbations by PMB, a cytotoxic membrane active peptide [14]. Adding PMB to biomimetic vesicles generated a striking colorimetric transition; and accordingly, a dominant peak appeared at ~540 nm, and a significant decline of peak was at ~650 nm (Fig. 5b) which demonstrated the strong interaction between PMB and model membrane.

Figure 5(a, b) shows that visible spectroscopy of the biomimetic vesicles was induced by sodium acetate–membrane interactions. The visible absorption spectra of the vesicle produced obvious changes when it encountered sodium acetate. When the color was changed, the absorption maximum at 650 nm was decreased with a concurrent absorption increase in the

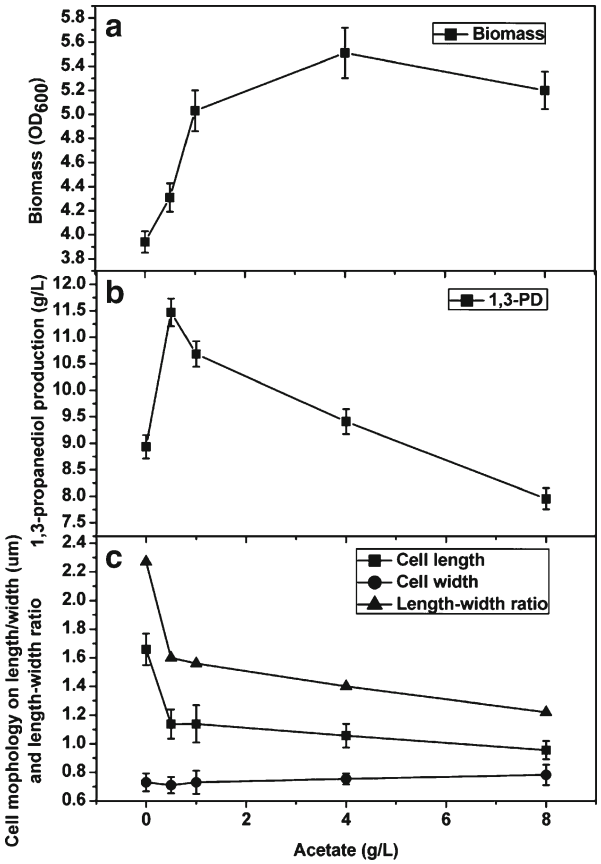

Fig. 4 Production of 1,3-propanediol by *K. pneumonia*e in shake flask without (control) and with addition sodium acetate. The data comprise biomass (**a**), 1,3-propanediol production (**b**), cell morphology on cell length/width, and the length–width ratio (**c**)

maximum at 550 nm in the visible absorption spectra. Our experiments thus demonstrated that the absorption maximum at 650 nm was significantly decreased with the additional sodium acetate as expected, while the absorption maximum at 550 nm was increased at a high concentration of additional sodium acetate. The quantitative analysis of sodium acetate with vesicle sensors was performed using spectroscopic measurements, and Fig. 6 shows the colorimetric response (CR). For acetate quantification, the CR was calculated: the percentage changed before and after sodium acetate incubation in the maximum absorption at 650 nm was normalized with the total absorption at both 650 and 550 nm. As shown in Fig. 6, the CR of PMB against the biomimetic vesicle reached 39 %. The CR of sodium acetate against the bimimetic vesicle was gradually increased with the additional sodium acetate. In addition, the CR was sharply increased by 71 % when the sodium acetate increased from 6.4 to 8.0 g/L.

Influence of Acetate Stress on Membrane's Fatty Acid Profile

There is also experimental evidence on a few model organisms that the composition of the cell membrane was impacted by acetate stress. Hence, the acetate treatments for their effect on fatty acid (FA) profiles of bacterial cells were assayed. Table 1 shows that the FA composition was

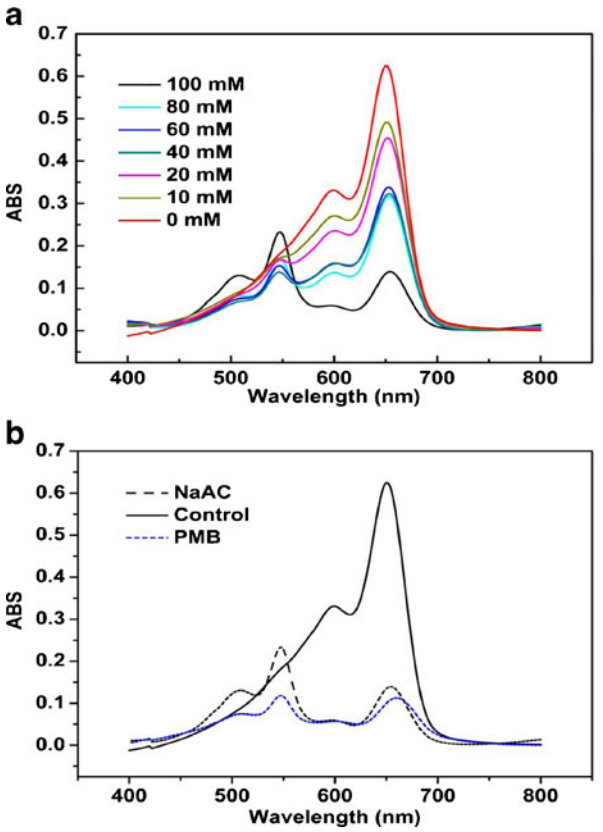

Fig. 5 UV–visible light absorption spectra of PDA-biomimetic vesicle induced by NaAC and PMB. **a** Interaction of vesicle with different concentrations of NaAC. **b** UV–visible light absorption spectra of PDA-biomimetic membrane in the presence of 8.0 g/L NaAC (*solid line*) and 250 μM PMB (*dotted line*)

significantly affected by the presence of acetate stress. Upon acetate (0.5 g/L) supply, the moderate changes to the overall composition were observed. There was an increase of the

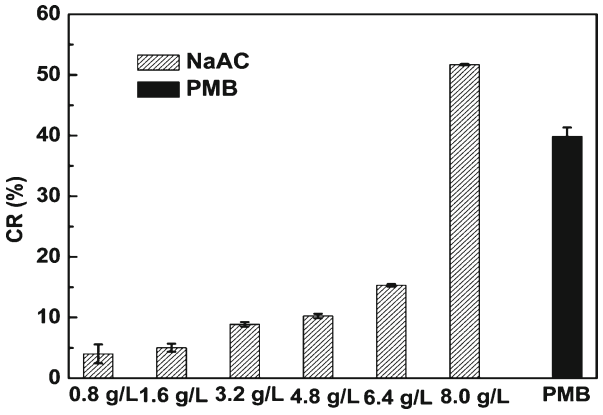

Fig. 6 Colorimetric responses induced by different concentrations of NaAC and PMB (250 μM). The experiments were carried out in triplicate to generate the error bars

Table 1 Changes in FA profiles of cell membranes of *Klebsiella pneumoniae* as induced by the addition of sodium acetate

NaAC addition (g/L)	0	0.5	8.0
C14:0	12.42±1.53	13.81±1.85	10.54±1.43
C16:0	41.90±0.90	41.80±1.27	37.64±2.03
C16:1^{9}	ND	1.48±0.02	2.4±0.37
C17:0 $^{\Delta 9}$	24.53±1.88	24.06±1.62	23.17±2.95
C18:0	4.56±0.07	3.58±1.10	7.09±0.89
C18:1	ND	ND	1.16±0.03
C18:2^{7,10}	ND	ND	5.03±0.28
C19:0 $^{\Delta 9}$	13.34±0.28	12.70±0.30	11.04±1.69
C20:0	4.69±0.51	ND	ND
TUFAs	0	1.48	8.59
TSFAs	63.57	59.19	55.27
TCFAs	37.87	36.76	34.21

Experiments were conducted in triplicate, and their mean values ±SD are presented*TUFAs* total unsaturated fatty acids, *TSFAs* total saturated fatty acids, *TCFAs* total cyclopropane fatty acids, *ND* not detected

unsaturated fatty acid (UFA) with 16 carbons at the expense of C14 saturated fatty acid (SFA), which was not detected in the control. Upon 8.0 g/L, the result showed a significant increase of UFAs with *cis*-9-hexadecenoate (C16:1), *cis*-9-octadecanoate (C18:1), and *cis*-7,10 octadecadienoate (C18:2), but a sharp decline in SFAs and cyclopropane fatty acids. Interestingly, the *cis*-7,10 octadecadienoate in the cell membrane was only observed upon the 8.0 g/L acetate stimulus.

Discussion

In view of the importance of cell morphology, it was worth manipulating the correct bacterial morphology for good performance in biotechnological process. While there are reports on morphological alterations in fungal fermentation, details of such alterations and their relationship with bacterial fermentation have not been studied. Interestingly, acetate affected the cell morphology of *K. pneumoniae* significantly, showing that a full range of morphological types formed from rod shape to oval shape even round shape which was dependent on acetate concentration.

To the best of our knowledge, this is the first report of a combined study of the metabolic and morphological phenotypes of an industrially important bacterial strain. It was found that the cell length became shorter and began to lose original shape with decreased length–width ratio upon the low level acetate addition, whereas the biomass and 1,3-PD production were improved significantly. Previous studies of acetate effects on 1, 3-PD fermentation only focus on the high-concentration acetate stress. Xue et al. 15] showed that the 1,3-PD production is inhibited when 10 g/L acetate is added to the fermentation medium. Cheng et al. [5] reported that the acetate is the main inhibitor metabolite during the 1,3-PD fermentation, while the critical concentration of acetate is 15 g/L. On the contrary, the positive results or phenomena have been observed in other studies. Lü et al. [16] studied the acetate effect on the product formation of fermenting polysaccharide-rich organic waste. They show that ethanol is favorably produced with acetate at pH 6, as well as the production of methanol and formate. He et al. examined the impact of elevated concentrations of acetate on ethanolic fermentation [17]. They show a stimulatory effect on ethanolic fermentation by *Thermoanaerobacter ethanolicus* with enhancing ethanol production by up to 394 %.

The growth of *K. pneumoniae* was stimulated by sodium acetate. Upon the acetate of 8.0 g/L supply, the biomass began to be decrease compared with 4.0 g/L acetate stimulus but increased by 32 % compared with the control. The main components of acid metabolites, $\Delta c_{\text{acetate}}$ and lactate both declined significantly with sodium acetate addition. The biosynthesis of main acid metabolites was strongly repressed under the sodium acetate stress. Generally, the growth inhibition by carboxylic acid is associated with the concentration of undissociated acid [18, 19] which is strongly pH dependent. Hence, the inhibition of acid pathway might contribute to the resistance to the acetate stress.

It should be also noted that *K. pneumoniae* could metabolize acetate. Figure 2 shows that the net acetate concentration declined from 1.98 to −2.62 g/L when additional acetate increased from 0 to 8.0 g/L, indicating the existence of the metabolic acetate pathways in *K. pneumoniae.* However, more efforts are required to investigate how and when they were metabolized by *K. pneumoniae*.

Due to the complexity of physiological membrane, few studies have investigated the inhibitor interactions associated with various aspects of membrane. Bioanalytical assays with high-throughput screening are increasingly important for identifying inhibitor involved in membrane interaction in industrial microbes. Here, we investigated the acetate stress on the membrane penetration of *K. pneumoniae* using a novel method of biomimetic vesicles. Initially, these data revealed an apparent relationship between the chromatic transitions and the mode of membrane penetration (Fig. 5b). A higher CR of PMB against biomimetic vesicle was observed that was ascribed to the membrane penetration of pore formation by PMB [20]. Figure 5a shows that there were obviously colorimetric changes when the sodium acetate was added to the biomimetic vesicle. Interestingly, sodium acetate that preferably interacts with the lipid head group region induced stronger color transitions, whereas deeper penetration into the hydrophobic lipid core generally resulted in more moderate blue-to-red transitions. Due to the low level acetate effect on 1,3-PD biosynthesis process, a limited penetration on cell membrane might accelerate the 1,3-PD biosynthesis. It is probably contributing to the similar and favored phenomena caused by other inhibitors in fermentation [21, 22]. However, the higher CR was gained at high concentration of acetate stimulus, while 1,3-PD metabolism was inhibited by the high stimulus.

Membrane phospholipids are important target chemicals because the lipids composition can display considerable variations with the environment chemical and physical properties [23, 24]. Given external perturbations, these modifications of membrane lipids are crucial for maintaining membrane fluidity, integrity, and functionality [25]. Previous studies show that membrane phospholipids are closely related to inhibitor tolerance in *Saccharomyces cerevisiae* [12]. There is also experimental evidence that acid tolerance is impacted by the composition of the cell membrane in organisms of the *Acetobacter* and *Glucanobacter genera* [26]. Therefore, the mechanism of defense toward the controlled membrane penetration at different levels of acetate was also investigated. According to our results (Table 1), acetate addition, in less membrane penetration, results in the increase in TUFAs/TSFAs ratio and the decrease in the TCFAs. When compared with high-level acetate addition, the TUFAs/TSFAs ratio was increased further and the TCFAs were decreased further. The increased TUFAs/TSFAs ratio revealed an increased fluidity of bacterial cell membrane. This increased fluidity inhibited the formation of stable pores in phospholipid bilayer. The increased membrane fluidity has been reported in *Bacillus cereus* LSPQ 2872 against γ-irradiation alone or in combination with mild heat or carvacrol treatment [27]. Moreover, the decreased TCFAs lead to an increased fluidity since their main function in bacteria is to increase membrane fluidity [12].

It requires modification of membrane fluidity for the proliferation of bacteria under suboptimal conditions, a phenomenon known as homeoviscous adaptation [28]. Membrane fluidity can be altered through modification of membrane FA profile [27] in order to ensure

vital functions, such as the maintenance of a proton-motive force or the active transport of metabolites [29].

As a successful utilization of the special acetate impact, our results demonstrated that cell morphology changes in response to limited membrane penetration by low-level acetate were valuable for 1,3-PD industrial production. These results will help in designing optimum medium composition and substrate feeding strategies as well as monitoring strategies via microscopic examinations.

Conclusions

This study showed that the acetate affected the cell morphology of *K. pneumoniae* significantly depending on the concentration of acetate. The cell growth and 1,3-PD productions in the shake flasks were improved evidently by the addition of 0.5 g/L acetate while the cell morphology formed shot-rod shape. The biomimetic vesicles composed of polydiacetylenes and cellular lipids from *K. pneumoniae* were constructed to investigate the cell membrane penetration by acetate, while higher concentration of acetate led to more moderate colorimetric transitions. The cell membrane's fatty acid profile in response to different levels of acetate was investigated, showing that the percentage composition was increased as well as the increased concentrations of acetate.

Acknowledgments This work was supported by the Key Program of the National Natural Science Foundation of China (no. 20936002) and the National Science Foundation for Distinguished Young Scholars of China (no. 21225626).

References

1. Kaup, B. A., Ehrich, K., Pescheck, M., & Schrader, J. (2007). *Biotechnology and Bioengineering, 99*, 198–491.
2. Zhang, Z. Y., Jin, B., & Kelly, J. M. (2007). *Engineering in Life Science, 7*, 490–496.
3. Selembo, P. A., Perez, J. M., Lloyd, W. A., & Logan, B. E. (2009). *Biotechnology and Bioengineering, 104*, 1098–1106.
4. Huang, H., Gong, C. S., & Tsao, G. T. (2002). *Applied Biochemistry and Biotechnology, 98–100*, 687–698.
5. Cheng, K. K., Liu, H. J., & Liu, D. H. (2005). *Biotechnology Letters, 27*, 19–22.
6. Nicolaou, S. A., Gaida, S. M., & Papoutsakis, E. T. (2010). *Metabolic Engineering, 12*, 307–331.
7. Jin, P., Li, S., Lu, S. G., Zhu, J. G., & Huang, H. (2011). *Bioresource Technology, 102*, 1815–1821.
8. Jelinek, R., & Silbert, L. (2009). *Molecular BioSystems, 5*, 811–818.
9. Kolusheva, S., Boyer, L., & Jelinek, R. (2000). *Nature Biotechnology, 18*, 225–227.
10. Dorosz, J., Gofman, Y., Kolusheva, S., Otzen, D., Ben-Tal, N., et al. (2010). *The Journal of Physical Chemistry B, 114*, 11053–11060.
11. Mehla, J., & Sood, S. K. (2011). *Applied and Environmental Microbiology, 77*, 786–793.
12. Xia, J. M., & Yuan, Y. J. (2009). *Journal of Agricultural and Food Chemistry, 57*, 99–108.
13. Ma, Z. F., Li, J. R., Liu, M. H., Cao, J., Zou, Z. Y., et al. (1998). *Journal of the American Chemical Society, 120*, 12678–12679.
14. Danner, R. L., Joiner, K. A., Rubin, M., Patterson, W. H., Johnson, N., et al. (1989). *Antimicrobial Agents and Chemotherapy, 33*, 1428–1434.
15. Xue, X. D., Li, W., Li, Z. M., Xia, Y. L., & Ye, Q. (2010). *Journal of Industrial Microbiology & Biotechnology, 37*, 681–687.
16. Lü, F., He, P. J., Shao, L. M., & Lee, D. J. (2008). *Biochemical Engineering Journal, 39*, 97–104.
17. He, Q., Lokken, P. M., Chen, S., & Zhou, J. Z. (2009). Characterization of the impact of acetate and lactate on ethanolic fermentation by *Thermoanaerobacter ethanolicus*. *Bioresource Technology, 100*, 5955–5965.
18. Beales, N. (2004). *Comprehensive Reviews in Food Science and Food Safety, 3*, 1–20.

19. Hüsemann, M. H. W., & Papoutsakis, E. T. (1988). *Biotechnology and Bioengineering, 32*, 843–852.
20. Orynbayeva, Z., Kolusheva, S., Livneh, E., Lichtenshtein, A., Nathan, I., et al. (2005). *Angewandte Chemie International Edition, 44*, 1092–1096.
21. Canovas, M., Bernal, V., Sevilla, A., & Iborra, J. L. (2007). *Biotechnology and Bioengineering, 96*, 722–737.
22. Ezeji, T., Qureshi, N., & Blaschek, H. P. (2007). *Biotechnology and Bioengineering, 97*, 1460–1469.
23. Hazel, J. R., & Williams, E. E. (1990). *Progress in Lipid Research, 29*, 167–227.
24. Sajbidor, J. (1997). *Critical Reviews in Biotechnology, 17*, 87–103.
25. Russell, N. J. (1984). *Trends in Biochemical Sciences, 9*, 108–112.
26. Hanada, T., Kashima, Y., Kosugi, A., Koizumi, Y., Yanagida, F., & Udaka, S. (2001). *Bioscience, Biotechnology, and Biochemistry, 65*, 2741–2748.
27. Yuk, H. G., & Marshall, D. L. (2004). *Applied and Environmental Microbiology, 70*, 4613–4620.
28. Sinensky, M. (1974). *Proceedings of National Academy of Sciences of the United States of America, 71*, 522–525.
29. Russell, N. J. (2002). *International Journal of Food Microbiology, 79*, 27–34.